Opposing spatial trends in methylmercury and total mercury along a peatland chronosequence trophic gradient

Baolin Wang[1], Mats B. Nilsson[2], Karin Eklöf[1], Haiyan Hu[3, 4], Betty Ehnvall[2], Andrea G. Bravo[5], Shunqing Zhong[6], Staffan Åkeblom[1], Erik Björn[7], Stefan Bertilsson[1, 4], Ulf Skyllberg[2], Kevin Bishop[1]*

[1]Department of Aquatic Sciences and Assessment, Swedish University of Agricultural Sciences, SE-75007 Uppsala, Sweden.

[2]Department of Forest Ecology and Management, Swedish University of Agricultural Sciences, SE-90183 Umeå, Sweden.

[3]State Key Laboratory of Environmental Geochemistry, Institute of Geochemistry, Chinese Academy of Sciences, 550081 Guiyang, China.

[4]Department of Ecology and Genetics, Limnology and Science for Life Laboratory, Uppsala University, SE-75236 Uppsala, Sweden.

[5]Department of Marine Biology and Oceanography, Institut de Ciències del Mar (ICM-CSIC). Pg Marítim de la Barceloneta 37-49, E08003 Barcelona, Catalunya, Spain

[6]College of City and Tourism, Hengyang Normal University, 421002 Hengyang, China

[7]Department of Chemistry, Umeå University, SE-90187 Umeå, Sweden.

*Corresponding author: huhaiyan@mail.gyig.ac.cn

ABSTRACT: Peatlands are abundant elements of boreal landscapes where inorganic mercury (IHg) can be transformed into bioaccumulating and highly toxic methylmercury (MeHg). We studied fifteen peatlands divided into three age classes (young, intermediate and old) along a geographically constrained chronosequence to determine the role of biogeochemical factors and nutrient availability in controlling the formation of MeHg. In the 10 cm soil layer just below the average annual growing season water table, concentrations of MeHg and %MeHg (of total Hg) were higher in younger, more mesotrophic peatlands than in older, more oligotrophic peatlands. In contrast, total mercury (THg) concentrations were higher in the older peatlands. Partial least squares (PLS) analysis indicates that the net MeHg production was positively correlated to trophic demands of vegetation and an increased availability of potential electron acceptors and donors for Hg methylating microorganisms. An important question for further studies will be to elucidate why there is less THg in the younger peatlands compared to the older peatlands, even though the age of the superficial peat itself is similar for all sites. We hypothesize that ecosystem features which enhance microbial processes involved in Hg methylation also promote Hg reduction that makes previously deposited Hg more available for evasion back to the atmosphere.

Keywords: peatland, mercury, methylation, methylmercury, chronosequence

1. Introduction

Methylmercury (MeHg) is a potent neurotoxin, and its bioaccumulation is a pronounced problem in high latitude aquatic ecosystems (AMAP, 2011; Loseto et al., 2004; Macdonald et al., 2005). Biological transformation from inorganic mercury (IHg) to MeHg predominantly occurs in anoxic ecosystems (Benoit et al., 2003; Compeau and Bartha, 1985; Gilmour et al., 2013). Peatlands are known to play an important role in the cycling of Hg in aquatic ecosystems; generally being sinks for total mercury (THg), but net sources of MeHg (Mitchell et al., 2008b; St. Louis et al., 1996;

43 Tjerngren et al., 2012b). MeHg generated in peatlands enters downstream aquatic ecosystems,
44 increasing the risk for harm to humans and wildlife that consume fish from these waters (Driscoll
45 et al., 1994; Munthe et al., 2007; Ratcliffe et al., 1996). The possibilities for mitigating and
46 managing this threat depends on knowing the environmental factors that control the formation of
47 MeHg.

48 Manipulation experiments have emphasized the dependence of net MeHg formation on the
49 availability of electron acceptors such as sulfate (Åkerblom et al., 2013; Branfireun et al., 2001;
50 Jeremiason et al., 2006; Mitchell et al., 2008a), electron donors in the form of high quality carbon
51 exudates from roots (Windham-Myers et al., 2009) and broader climate effects (Bergman et al.,
52 2012). Manipulation experiments, however, are sometimes difficult to generalize to natural
53 environments because of artefacts, such as unintended disturbance effects or the generally limited
54 duration of manipulations. As a complement, field studies along natural gradients have been used
55 to verify experimentally determined factors controlling Hg methylation in peatlands, including
56 sulfate and nutrients. Such studies have generally shown that methylation increases with increasing
57 sulfur and/or nutrient availability to a certain point, beyond which more nutrients and/or sulfur
58 lead to less MeHg (Gilmour et al., 1998; Tjerngren et al., 2012a). In such field studies, though,
59 geographic differences in climate and management history can complicate interpretations of
60 causality.

61 An ecosystem chronosequence within a restricted geographical area represents a model system
62 that avoids most drawbacks in comparison to more geographically distributed experimental
63 locations. Isostatic rebound since the last glaciation, which continuously raises the coastline
64 around the Gulf of Bothnia between Finland and Sweden at a rate of around 8.2 mm per year
65 (Hünicke et al., 2015), has created chronosequences of boreal ecosystems that can span up to 10000

66 years within restricted areas. The major differences between younger and older peatlands across
67 such a chronosequence are increasing peat depth and peatland area with peatland age, together
68 with decreasing delivery of weathering products from the watersheds that deliver dissolved
69 minerals to the older peatlands. All these three factors generate biogeochemical and ecological
70 differences between younger and older peatlands. The biogeochemically active upper decimeters
71 of all the peatlands in the chronosequence, however, have similar ages (several decades).
72 Compared to the surface of the "younger" peatlands, the surface of "older" peatlands on the
73 chronosequence are expected to have lower availability of elements originating from mineral
74 substrates, including all plant nutrients except for nitrogen. This is reflected in significant
75 differences in the plant community composition, with more nutrient demanding vegetation on the
76 younger peatlands (Tuittila et al., 2013). Thus factors which influence the biogeochemistry of
77 significance for mercury biogeochemistry, including potential electron acceptors and donors, as
78 well as plant communities can be expected to vary systematically along a peatland
79 chronosequence. This facilitates studies of long-term biogeochemical influences, and related
80 vegetation changes on the net formation of MeHg without introducing experimental manipulations
81 that would need to be maintained for decades.
82 In this study, a chronosequence was used to test the hypothesis that net MeHg formation in the
83 surface peat soil along the chronosequence peatlands would change with trophic status as indicated
84 by the availability of minerogenic elements and the quality of organic matter for Hg methylating
85 microorganisms. Those ontogenetic changes would involve both a decrease in major electron
86 acceptors such as sulfate and Fe(III), as well as a concomitant decrease in electron donors
87 (represented by organic matter quality characteristic of the vegetation composition) with
88 increasing peatland age. These differences would exist despite all of the superficial peat layers

sampled along the chronosequence being exposed to a similar climate and atmospheric Hg deposition for a similar period of time. Fifteen peatlands were selected for the study in order to provide sufficient material to resolve the influence of specific environmental factors on Hg cycling and MeHg formation.

2. Materials and methods

2.1. Site description

Post-glacial land uplift in northern Sweden along the Gulf of Bothnia has created a landscape with many peatlands along an age gradient spanning from 0 to > 4000 years within < 10 km from the sea. Peatland age since its initiation was obtained according to the shoreline displacement curve for southern Västerbotten that was based on ages dated by the varve-counts of lake sediments and the present-day sea level (Renberg and Segerström, 1981).

The topographic relief of the area is quite low, with small areas of mineral soil up to a meter higher than the peatland. The superficial groundwater tables (ca 10 cm depth on average) have a decimeter of annual variation around the mean. The low topographic relief and the groundwater levels are indicative of a superficial flow system with little regional influences. In this landscape, regional land uplift from the sea creates the conditions for peat to form on what used to be the seabed. Then the growth of that peat successively separates the superficial peat from the underlying sources of minerogenic elements, with lateral minerogenic inputs only from the local “uplands”. The degree of this input is reflected in the unique catchment to peatland ratio (Table S1, Figure S3 in the Supplementary material (SM)).

An initial vegetation survey of seventy peatlands along the chronosequence was conducted by performing an agglomerative hierarchical clustering of vegetation data (e.g. species and relative species abundance), in which Ward’s linkage method and Euclidean distance were used as a group

112 linkage method and a distance measure, respectively. Six vegetation classes (1 - 6) were clearly
113 clustered, with the increasing number value representing more nutrient demanding vegetation
114 composition (Table 1). Fifteen open peatlands were then selected from three age classes, young (<
115 10 m.a.s.l, < 1000 years, n = 5), intermediate (10 - 20 m.a.s.l, 1000 - 2000 years, n = 5) and old
116 (20 - 40 m.a.s.l, > 2000 years, n = 5) (Figure 1). The three peatland age classes were clearly
117 different with respect to elevation, soil acidity (pore water pH), and vegetation composition (Table
118 1, Table S2 (vegetation)).

119 *2.2. Sampling and Sample Preparation*

120 Four sampling campaigns were carried out in June and August of 2016 and 2017. In June 2016,
121 five 70 × 70 cm plots were established within each of the fifteen peatlands. The five plots within
122 each peatland were located at least 5 m away from each other along a line across the center of the
123 peatland. A cube-shaped core of peat soil (10 × 10 × 10 cm) was extracted from each plot of each
124 peatland with a long (60 cm), sharp, custom-made knife. The top of the peat core was defined by
125 the level of the average growing season ground water table (GWT) from the peat soil surface of
126 each peatland. The average GWT ranged from 8.7 cm depth below the soil surface in the young
127 peatlands, to 9.4 cm depth in the intermediate peatlands, and 13.6 cm depth for old peatlands,
128 respectively (Figure S1). The sampled peat core was cut into upper and lower layers (0 - 5 and 5 -
129 10 cm, respectively). These samples were then sealed in separate plastic zip-lock bags after the air
130 was squeezed out. All the samples were kept in a dark cooling box during transport and stored in
131 a refrigerator at 4 °C for up to two weeks until further sample preparation. In 2016, the pH was
132 determined in the porewater that immediately refilled the sample hole. While in 2017, the pH was
133 determined in the porewater of the 10 cm peat core that was sampled with a 70 cm long, custom-
134 made, Teflon sampler (Bergman et al., 2012).

All the five upper layers (0 - 5 cm) taken in the same peatland were homogenized in fresh state through a 4 mm cutting sieve and merged to one composite sample. The homogenization was done after removal of bulky roots, sticks and living plant material. The same was then done for the lower layers (5 - 10 cm). Immediately after homogenization, approximately 50 g of fresh peat soil was taken and frozen for subsequent determination of MeHg concentration. Triplicate subsamples were taken for the determination of water content by heating at 105 °C until constant mass was achieved. Another ~ 200 g of subsample was dried at 40 °C until the peat mass was constant. The low temperature was selected to avoid losses of elemental mercury (Hg(0)) (Kodamatani et al., 2017). Dried peat subsamples were used for analysis of concentrations of THg and other elements (e.g. C, N, S) after ball milling (vibrated at 30 Hz for 5 min, Retsch MM400, Retsch GmbH, Germany).

2.3. Chemical Analyses

The THg in the peat soil dried at 40 °C was analyzed by solid combustion atomic absorption spectrometry (DMA-80, Milestone, Italy) using certified marine sediment reference material MESS-3 (National Research Council of Canada, 0.091± 0.009 mg Hg kg^{-1}) for calibration. The MeHg content in fresh peatland soils was determined by isotope dilution analysis described in detail elsewhere (Lambertsson et al., 2001; Tjerngren et al., 2012a). Concentration of IHg was calculated by subtracting MeHg from THg. The percentage of MeHg to THg (%MeHg) in the solid peat was also calculated. While the MeHg level itself is of interest for what is transferred from peatlands into downstream ecosystems, the %MeHg in the peat is a better indicator of the net methylation potential (Drott et al., 2008).

Total concentrations of C and N were analyzed on an Elemental analyzer (Flash EA 2000, Thermo Fisher Scientific, Bremen, Germany). Total concentrations of Ca, Fe, Mg, Mn, Na, K, Al, Zn, Si, S and P were determined by ICP-OES (Spectro Ciros Vision, Spectro Analytical

158 Instruments Inc., Germany). These parameters measured by ICP-OES and Elemental analyzer
159 were only measured on both of the two sampling occasions in 2016, but not in 2017 as we assumed
160 that the values did not change between 2016 and 2017. Replicate samples and reference material
161 were analyzed regularly and the precision was under 10% relative standard deviation (RSD).

162 *2.4. Topographical Data*

163 A 2 × 2 m national gridded digital elevation model (DEM) was used to extract hydrological and
164 geomorphological features of the peatlands and their contributing catchments. The high-resolution
165 DEM was generated by the Swedish Mapping, Cadastral and Land Registration Authority
166 (Lantmäteriet) from a LiDAR point cloud with a point density of 0.5 - 1 points m^{-2}, a vertical
167 resolution of 0.3 m and a horizontal resolution of 0.1 m. The DEM was preprocessed prior to the
168 hydrological modelling by burning stream-road intersections and breaching depressions. Flow
169 direction and accumulation were calculated using the deterministic eight-direction flow model
170 (D8) (O'Callaghan and Mark, 1984). All hydrological modelling was performed in Whitebox
171 Geospatial Analysis Tools. The morphological modelling was based on the original DEM and
172 performed in SAGA GIS 6.2.0. Topographic indices used to describe the peatlands and their
173 catchments are documented in Table S1.

174 *2.5. Statistical Data Analysis*

175 Normality and homogeneity of the data were checked using the Shapiro-Wilkinson test prior to
176 statistical analyses. Log transformation was used to meet the parametric test for normality when
177 the original data were not normally distributed. All the parametric significant differences (e.g.
178 THg, MeHg and %MeHg) across the fifteen peatlands on the four sampling occasions at the two
179 sampling depth (0-5 cm and 5-10 cm below the GWT) were tested by three-way ANOVA,
180 followed by Tukey's multiple comparison test. The three factors tested were peatland type (3 age

classes), sampling depth and month of sampling (June and August). All these tests were carried out at the 0.05 significance level using R (Version 3.6.0). All the statistical tests involving element concentrations (e.g. total C, N, S) from the ICP-OES were carried out with the average values of the two 5 cm layers for each peatland on each of the two sampling occasions in 2016. Principle Component Analysis (PCA) and Partial Least Square (PLS) analysis, on non-GIS data, were conducted in the SIMCA software package (Version 14, Umetrics Umeå, Sweden), using only data from the two sampling occasions in 2016. The PCA of GIS data, including average %MeHg of the two 5 cm layers of all the four samplings during 2016 – 2017 for each peatland, were conducted using R (Version 3.6.0).

3. Results

3.1. Characteristics of the Chronosequence of Peatlands

The three age classes along the chronosequence exhibited clear distinctions in vegetation composition and several other geochemical and geomorphological features of the study peatlands that related to the trophic status (Table S2 and Table S3). These differences and relationships are evident from the principle component analysis (PCA) (the first two components, $R^2X = 60\%$, $Q^2 = 40\%$). The first principle component (PC1, 43% of total variance) separated old peatlands (positive scores on PC1) from young peatlands (negative scores on PC1), with intermediate peatlands having either positive or negative scores on PC1 (Figure 2a). The old peatlands, situated at higher elevations above sea level, were slightly more acidic (average porewater pH 3.8 ± 0.2; Table S3) and nutrient poor (oligotrophic) than the younger peatlands, as characterized by short growing sedges (*Eriophorum vaginatum*, *Trichophorum* spp. and *Carex limosa*), dwarf shrubs (*Andromeda polifolia* and *Vaccinium oxycoccus*) and *Sphagnum majus*, *Sphagnum balticum* and *Sphagnum papillosum*, in the field- and bottom-layer, respectively (Table S2). The old peatlands had lower

concentrations of most minerogenic elements (e.g. Mg, Mn, Fe, K, Na) (negative loadings on PC1) relative to the young and intermediate peatlands (Figure 2b). The lower minerogenic influence on the old peatlands was also reflected in higher concentrations of C in the superficial peat soil (Table S3) and greater peat depth (Table 1). In contrast, young peatlands were less nutrient poor, i.e. mesotrophic, with relatively higher porewater pH (4.3 ± 0.5) and higher minerogenic element concentrations and vegetation classes that require more nutrients to thrive and spread (Figure 2b and Table S3). The vegetation is characterized by *Carex rostrata*, *Eriophorum vaginatum* and some herbs (e.g. *Potentilla palustris*) in the field layer and *Sphagnum squarrosum*, *Sphagnum fallax* and *Sphagnum riparium* in the bottom layer (Table S2). The intermediate peatlands were intermediate with regards to trophic status, biogeochemistry and vegetation composition.

The younger peatlands were separated from old and intermediate peatlands with regards to hydrological and geomorphological properties (Figure S3). Peatland and catchment morphological properties (i.e. topographic wetness index (TWI), Elevation above stream (EAS), downslope index (DI), catchment slope, peatland curvature) were some of the features separating young peatlands from old peatlands along the first principal component (29.4 % of total variance).

3.2 Overall effects on THg, MeHg and %MeHg

The three-way ANOVA models, considering peatland type (three age classes), sampling depth (two classes) and month (two classes) explained 37%, 21% and 38% of the variance for THg, MeHg and %MeHg respectively (Table 2). Only the main factors peatland type and layer depth contributed significantly to the models (Figures 1 and S2). None of the interaction terms were significant. The variations in concentrations of THg, MeHg and %MeHg were significantly explained by peatland age class and the variations in THg and MeHg were also additionally explained by peat layer depth.

227 *3.2. Concentrations of THg in Peat Soil*

228 The old peatlands had higher THg concentrations on all sampling occasions in 2016 and 2017
229 (average THg of 0 - 5 and 5 - 10 cm layers, 77.2 ± 26.4 ng/g dw, $p < 0.05$, Tukey's multiple
230 comparison test) compared to young (43.6 ± 15.8 ng/g) and intermediate peatlands (57.5 ± 24.1
231 ng/g). However, there were no statistical differences between young and intermediate peatlands in
232 this regard (Figure 3a and Table S3).

233 The PLS model of the spatial and temporal variation in THg from the two sampling occasions
234 in 2016 could, with the first two principle components (R^2X = 58%) together, explain 85% (R^2Y)
235 and predict 80% (Q^2) of the variation in THg across the chronosequence of the fifteen peatlands
236 (Figure S5a). Variable importance for the projection (VIP) plots summarize the importance of the
237 explanatory variables (X) for the response variable(s) (Y), with VIP-values larger than one
238 indicating "important" X-variables. The important variables of the PLS model for THg were K,
239 C/N, elevation, S, C, Mg, Al, and vegetation class (Figure 4a). The explanatory variables having
240 a significant positive correlation with THg concentrations included those that were characteristic
241 for old peatlands, such as high C concentrations and elevation. In contrast, those that were high in
242 the younger peatlands, such as Mg, Mn, Ca, Na, pH and more nutrient demanding vegetation
243 classes characterized by herbs and tall sedges, correlated negatively with THg (Figure S5a).

244 *3.3. Concentrations of MeHg in Peat Soil*

245 MeHg concentrations were higher in young peatlands (average MeHg of 0 - 5 and 5 - 10 cm
246 layers, 4.0 ± 3.2 ng/g dw) than in old peatlands (2.5 ± 1.6 ng/g), with no difference between young
247 and intermediate ones (3.4 ± 1.8 ng/g) or between intermediate and old ones (Figure 3b, Table S3).
248 While month of sampling was not significant (Table 2), there was more variation in MeHg
249 concentrations in August, 2016 (wet summer, higher GWT, precipitation during June and August

250 = 231 mm) compared to August, 2017 (dry summer, lower GWT, precipitation during June and
251 August = 175 mm) (Table 1, Figure S1, Figure S6).

252 The PLS model with MeHg as dependent variable explained 69% of the variance in MeHg
253 concentrations with the first two PLS-components (R^2X = 52%, Q^2 = 38%; Figure S5b). The
254 variables with the highest VIP in this model were Zn, GWT, Ca, pH, Fe and Mg (Figure 4b). The
255 concentration of MeHg was positively correlated to variables high in young peatlands (e.g. pH,
256 Ca, Fe, S, Mg, Mn) and negatively correlated to those characteristic for old peatlands (e.g. high
257 elevation, C and IHg) (Table S3, Figure S5b). Interestingly, P and Zn, which were not statistically
258 different across the three age classes of peatlands (Table S3), correlated positively and negatively
259 with MeHg respectively (Figure S5b).

260 *3.4. %MeHg in Peat Soil*

261 Similar to MeHg, %MeHg was higher in young (average %MeHg of 0 - 5 and 5 - 10 cm layers,
262 10.9 ± 10.7 %) and intermediate peatlands (7.2 ± 4.8 %) than in old peatlands (3.2 ± 1.9 %), with
263 no difference between young and intermediate peatlands (Figure 3c, Table S3). While there was
264 no statistical difference in %MeHg (Table 2), there was more variation in August 2016 (Figure
265 S7a) compared to August 2017 (Figure S7b).

266 Using %MeHg as the response variable resulted in a substantially stronger PLS model (the first
267 two components, R^2X = 54%, R^2Y = 82%, Q^2 =62%) than for MeHg. The relatively higher Q^2-value
268 also indicates a more robust model than for just MeHg (Figure S5c). The important variables for
269 the projection in this model were Zn, K, Mg, Ca, pH, IHg, C, Mn, vegetation class and elevation
270 (Figure 4c). The relationship between the explanatory variables and the independent variable here
271 (i.e. %MeHg) was similar to that of the MeHg PLS-model with positive correlations to pH, K, Ca,
272 Fe, Mg, Mn and negative correlations to C and IHg (Figure S5c). The concentrations of Zn, which

were not significantly different along the three age classes (Table S3), correlated strongly and negatively with %MeHg (Figure S5c).

The PCA of GIS data, including average %MeHg of the two 5 cm layers of all the four samplings during 2016 – 2017 for each peatland, showed that catchment topographic position index 500 (TPI500), peatland DI and EAS correlated negatively with %MeHg, while peatland TWI correlated positively with %MeHg, indicating a hydrological influence on net MeHg concentration (Figure S3). Apart from these indices, peatland and catchment elevation as well as age correlated significantly with %MeHg, which was already clear in Figure 2.

4. Discussion

The peatland chronosequence provides a natural gradient of trophic status and hydrogeochemistry due to the successive isolation of the peat surface from mineral substrates caused by the increasing peat depth, increasing lateral extent of peatland area and decreasing weathering rates in the watershed as peatland age. This increasing isolation of the vegetation growing each year at the peatland surface explains why increasing peatland age correlated with declining concentrations of minerogenic elements such as Mn, Mg and Fe. These elements are derived primarily from the mineral parent material on which the peat grows, or runoff of weathering products from the surrounding catchment. (Figure 2, Table S3). This decline in minerogenic elements also coincided with a lower pH and declining nutrient availability with age along the chronosequence, as reflected by the change in vegetation composition (Table S2). Along this trophic gradient, both MeHg concentrations and apparent Hg net methylation potential (%MeHg) in the solid peat were higher in the young and mesotrophic peatlands compared to the old and oligotrophic peatlands (Figure 3, Table 2). This is in agreement with our main hypothesis

295 that MeHg formation will be stimulated in more nutrient-rich peatlands, i.e. mesotrophic peatlands
296 in this study, due to higher nutrient availability to Hg methylating microbes.

297 The ontogenetic changes in net MeHg formation along this chronosequence of varied trophic
298 status may be due to changes in the activity of Hg methylating microorganisms, mainly including
299 sulfate-reducing bacteria (SRB), iron-reducing bacteria (FeRB), methanogens, syntrophs, and
300 *Firmicutes* (Compeau and Bartha, 1985; Fleming et al., 2006; Gilmour et al., 1992; Gilmour et al.,
301 2013; Hamelin et al., 2011; Kerin et al., 2006; Wood et al., 1968; Yu et al., 2018). Our study
302 focused on the 10 cm of peat soil sampled immediately below the average growing season GWT.
303 This is an area where water table fluctuations create redox oscillations likely to favor microbial
304 processes such as reduction of sulfate and ferric iron, both of which are implicated in Hg
305 methylation (Bergman et al., 2012), and where organic matter degradations, for example by
306 syntrophs (Bae et al., 2014; McInerney et al., 2009; Stams and Plugge, 2009; Yu et al., 2018),
307 occur offering electrons to Hg methylating microbes. In the young peatlands higher concentrations
308 of potential electron acceptors such as iron (when oxidized) (Bravo et al., 2018) (Figure 2 and
309 Table S3) as well as more potential sources of electron donors in labile organic matter of root
310 exudates from vascular sedges (Haynes et al., 2017; Windham-Myers et al., 2009) (Table S2) could
311 stimulate higher methylator activity, leading to the higher net MeHg formation observed in the
312 young peatlands.

313 We analyzed the upper and lower 5 cm of this 10 cm layer below the average GWT separately,
314 and the concentrations of both MeHg and THg were somewhat greater in 5-10 cm layer compared
315 to 0-5 cm layer (Figure S2). There was, however, no difference in the %MeHg between the two
316 layers (Table 2). There were also no depth differences in organic matter quality (C/N ratio) or
317 concentrations of minerogenic elements (data not shown). Furthermore, there were also no

differences in THg, MeHg and %MeHg between the June and August samplings (Table 2). This suggests that other than the depth differences in MeHg and THg, there were no distinct vertical gradients in the net methylation potential within the decimeter below the annual mean growing season GWT, or major temporal differences in the studied parameters during the snow-free season.

The finding that Hg net methylation potential (%MeHg) was lower in the more oligotrophic, old peatlands is in agreement with previous research demonstrating that nutrient status influences net MeHg production, with a peak in production at intermediate nutrient availability (Tjerngren et al., 2012b). However, this optimal nutrient level is not surpassed in the chronosequence studied here, as these only cover the lower range (acidic part) of the nutrient gradient (Table S3).

The change in apparent Hg net methylation potential with indicators of wetness, which also correlate with age and trophic status, is reflected in the GIS derived landscape characteristics (Figure S3, Table S1). The correlations with TWI, DI and EAS of peatlands suggest that Hg methylation is a function of wetness where a higher average peatland wetness (high TWI, low DI, low EAS) leads to a higher methylation potential.

One additional factor that could promote Hg methylation is the presence of a large pool of Hg. There was, however, a negative relationship between %MeHg and IHg across the peatland chronosequence (Table S3, Figure S5c). Hence higher IHg does not seem to promote Hg methylation in these ecosystems, leading us to conclude that other factors such as methylator/demethylator activity and the availability of specific Hg species control net Hg methylation. This result agrees with other studies that have not found bulk Hg as a factor controlling methylation (Åkerblom et al., 2013; Branfireun et al., 2001).

The difference in THg in the superficial peat along this peatland chronosequence raises the question of a causal mechanism. Even though the peatlands at 20 - 40 m elevation are thousands

of years older than those closer to sea level, the actual age of the peat being sampled just below the GWT is expected to be similar (several decades) for all of the sampled peatlands. Thus the sampled peat material should have been exposed to the same Hg deposition and atmospheric concentrations independent of peatland age. It must therefore be something about the environment of the younger peats that either prevents accumulation of Hg or removes deposited Hg from the surface peat, either back to the atmosphere or to the downstream aquatic ecosystems.

Peat decomposition indicated by bulk density and C/N ratio of peat is suggested to influence Hg retention (Biester et al., 2012; Rydberg et al., 2010), but there was no statistical difference in bulk density or C/N ratio between the three peatland classes (Table S3). This suggests that peat decomposition is not responsible for the differences in Hg concentrations between the three peatland classes along the chronosequence. Vegetation type and composition can also affect both Hg concentration and long-term accumulation in peatlands. It has been reported that open *Sphagnum* fens have lower Hg concentrations and net accumulation than pine-covered fens and that *Sphagnum* mosses sequester more Hg compared to vascular plants (Rydberg et al., 2010). In this study, all sites are open *Sphagnum* areas, so tree cover should not be a factor. The young peatlands have a denser cover of vascular plants compared to old peatlands (Table S2), so this may contribute to less THg in the young peatlands, even though sphagnum is the main vegetation at all sites.

Jiskra et al.(2015) have inferred Hg evasion from organic forest soils within 100 km of our study area based on the isotopic signature of the soils. Furthermore, the first full year measurement of land-atmosphere exchange over a peat bog (further inland from the chronosequence in this study) has demonstrated Hg evasion back to the atmosphere at a rate three times higher than the rate of wet deposition (Osterwalder et al., 2017). This establishes that net Hg(0) evasion is possible,

possibly as a response to declines in regional atmospheric Hg(0) concentrations of 50% since the 1980s (Streets et al., 2011). However, the abovementioned micrometeorological study was carried out on a single peatland at the old and nutrient poor end of the spectrum included in the current study, and does thus not inform us about how evasion rates may vary with nutrient status.

Advective losses of Hg associated with water moving through and out of peatland ecosystem also occur. However, the precipitation (and presumably runoff) is similar across all the sites (Table 1), so it would need to be concentration differences in the advective flows that could explain the age-related differences. Furthermore, the Hg evasion was also seven times greater than stream Hg export from the peatland where Hg evasion was measured (Osterwalder et al., 2017). If higher THg in old peatlands in this study is a result of less evasion from older peatlands than younger peatlands along the chronosequence during recent decades, then it suggests that the same factors that promote Hg methylation may also promote Hg(0) evasion. In fact, a decade of experimental sulfate addition to a part of that older peatland where the micrometeorological study was conducted (Osterwalder et al., 2017), significantly reduced the THg in the peat (Åkerblom et al., 2013), while at the same time stimulating methylation during much of the growing season.(Bergman et al., 2012)

Assuming that all of the observed difference in THg content of young and old peatlands in the peat layer 0-10 cm below the GWT was due to evasion over the past 30 years from only that layer, then the difference in Hg content between the old peatlands (263 $\mu g/m^2$) and the young peatlands (102 $\mu g/m^2$) could be explained by 5.4 $\mu g/m^2$/year more evasion from the younger peatlands, relative to the older peatlands. The evasion from the younger peatlands would be in addition to any evasion from older peatlands. The net Hg evasion rate from an older peatland in the region was 10 $\mu g/m^2$/year during 2013-2014 (Osterwalder et al., 2017).

Reduction of oxidized Hg(0) was also suggested to be a key factor in the evasion of Hg from that peatland studied by Osterwalder et al. (2017) who observed a temporal correlation between evasion of Hg from the peat surface and the concentration of dissolved gaseous Hg in the peatland porewater just below the water table. If microbial reduction of oxidized Hg were a feature of this environment, this could explain both the evasion of Hg that is reduced to Hg(0) and increased Hg methylation potential (as oxidized IHg is rendered available for methylation) in the younger peatlands. Microbial Hg(0) formation can occur under dark and anaerobic conditions by dissimilatory metal-reducing bacteria (Hu et al., 2013; Wiatrowski et al., 2006), and some of them (e.g. *Geobacter sulfurreducens*) are also known to be capable of methylating Hg (Schaefer and Morel, 2009). The activity of such bacteria could be stimulated by the higher concentrations of electron acceptors such as ferric iron and some other elements observed in the younger peatlands together with more labile root exudates of organic matter expected from the more productive vegetation composition in younger peatlands (Table S2, Table S3) (Åkerblom et al., 2013; Windham-Myers et al., 2009; Yu et al., 2012). Furthermore, the incubation experiments in Hu et al. (2020) with samples from three of the peatlands in this study showed that the rates of both Hg methylation and MeHg demethylation were highest in the younger peatland, setting up conditions that might not only fuel the growth of microbes but also make Hg more available for Hg reduction to elemental Hg back to the atmosphere. This would be consistent with higher re-emission of Hg(0) from young peatlands as well as the promotion of Hg methylation in these systems.

The results from this study contribute to a better understanding of the large scale patterns of Hg accumulation and Hg evasion from peatlands in both space and time, and also inform us about characteristics that are likely to promote Hg methylation and Hg evasion. The inverse relationship between net MeHg production and THg content of peat along the chronosequence of peatlands is

410 striking. These ecosystems have been exposed to similar Hg deposition and climate for centuries,
411 enabling us to map differences in biogeochemical pathways of Hg cycling as peatland age. We
412 propose that future research on Hg transformations in the boreal landscape could benefit from
413 quantifying the Hg evasion rates along these MeHg formation gradients as well as combining
414 isotopic and genomic approaches for better understanding of the mechanisms behind the interplay
415 between MeHg formation and Hg evasion.

416 **Supporting Information**

417 Supporting Information contains 7 figures and 3 tables, specifically on ground water table,
418 description of morphological and topographical indices, differences in THg, MeHg, and %MeHg
419 between 0-5 and 5-10 cm layers, vegetation composition, chemical parameters of peat soil, PCA
420 of the topographic indices, PLS analyses for THg, MeHg and %MeHg, as well as differences in
421 THg, MeHg, and %MeHg between June and August samplings.

422 **Acknowledgments**

423 This work was supported by the China Scholarship Council (CSC, 2015-2018), the Sino-
424 Swedish Mercury Management Research Framework (SMaReF: VR2013-6978), the National
425 Natural Science Foundation of China (No.41573078 and 41303098) and the Swedish research
426 council FORMAS (2106-00896). Thanks to Tao Jiang, Nguyen Liem, Yu Song and Wei Zhu for
427 their assistance in the laboratory. Thanks to Lucas Perreal, Camille Guyenot, Thibaut Imbert,
428 Edward van Westrene, Marloes Arens, Mélissa Garsany, Laura Manteau, Jeanne Latour, Charles
429 Sanseverino, Quan Zhou and Itziar Aguinaga Gil for the help with the field work.

Graphical abstract

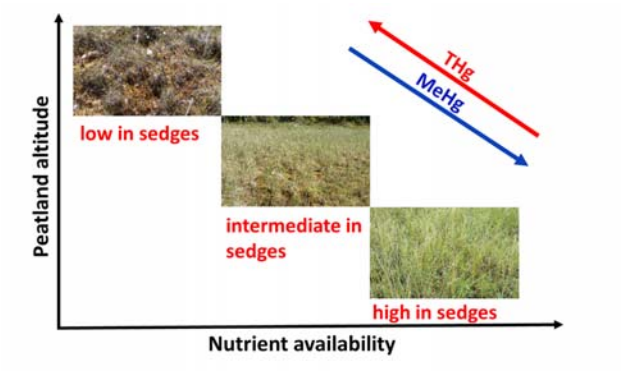

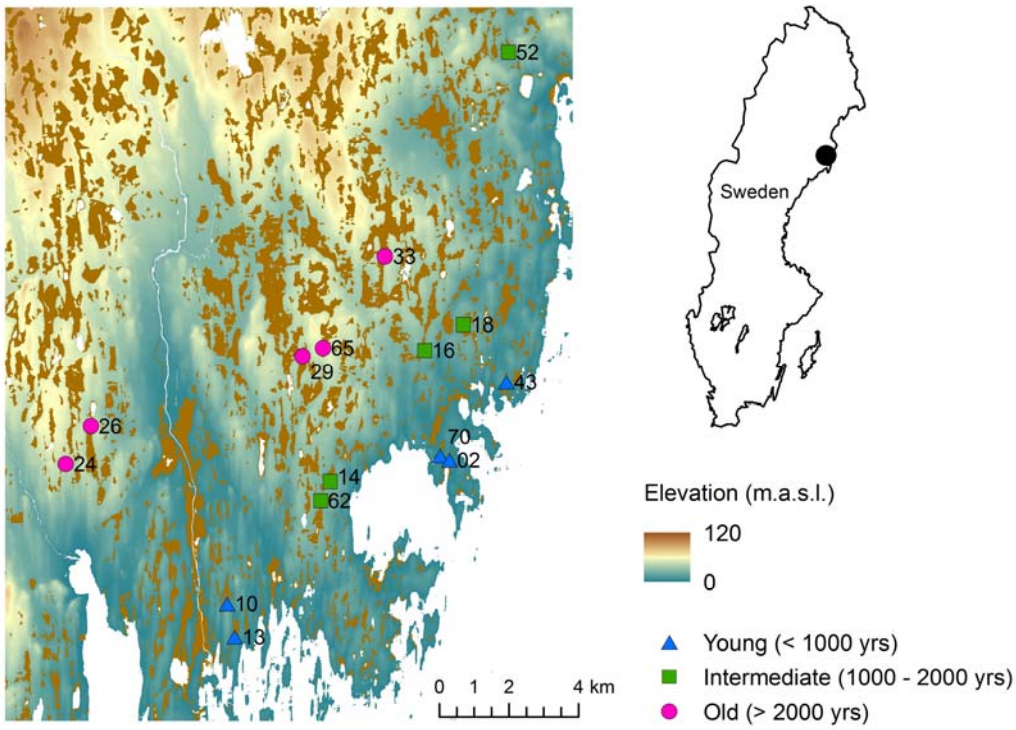

Figure 1. The peatland sampling sites located on the northeast coast of Sweden where post-glacial uplift has created a relationship between elevation above sea level and the age of the peatland. The color of the symbol marking each sampling site indicates the age class (blue triangles = young, green boxes = intermediate, and pink dots = old) assigned to the peatland in this study. The numbering relates to an initial vegetation inventory of some seventy peatlands along this chronosequence.

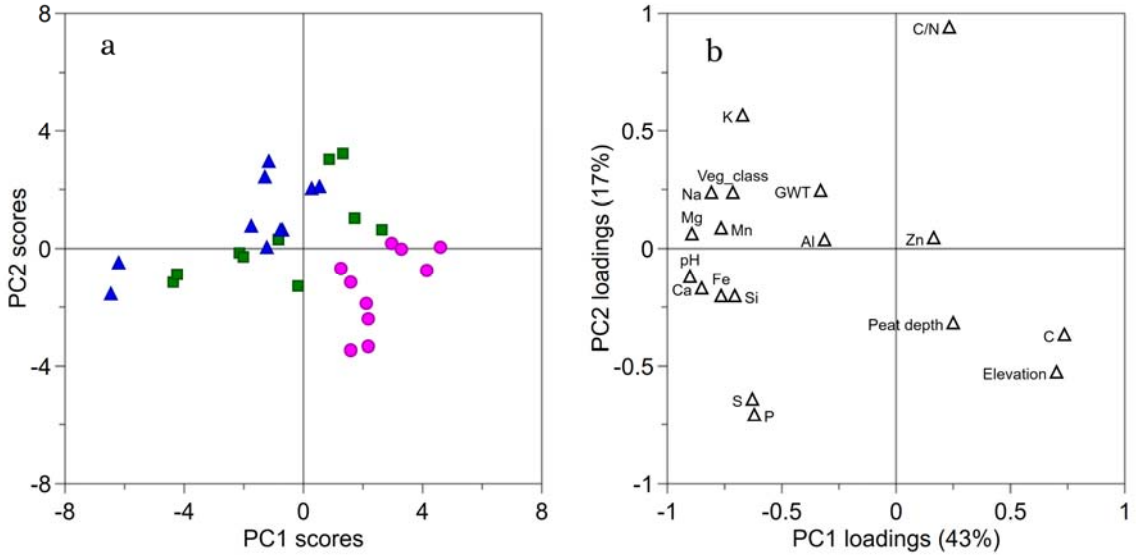

Figure 2. PCA of the explanatory variables (biogeochemistry and vegetation) measured on two sampling occasions during 2016 along a chronosequence of fifteen peatlands. (a) Scores for the three age classes of peatlands, young (blue triangles), intermediate (green boxes) and old (pink dots); (b) Variables strongly contributing to separate the old and young peatland classes have high or low loading respectively for PC1, reflecting the gradient of nutrients and related factors created by peatland aging. It should be noted though, that by sampling the peat immediately below the water table, the age of the peat layer sampled at all sites was similar. Whether the peatland was established 200 years ago or 2000 years ago, the peat material just below the water table is decades old. It is separation from the mineral substrate that increases with age as well as decreasing weathering in any surrounding catchment that differs between the age classes.

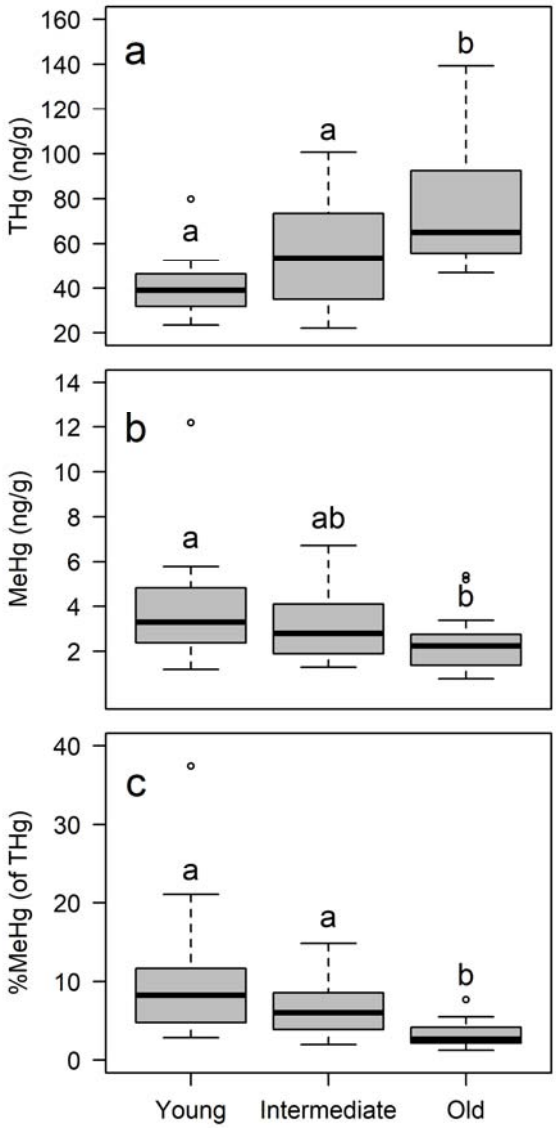

Figure 3. THg (a), MeHg (b) and %MeHg (c) of the 10 cm peat samples collected on four sampling occasions (June and August, 2016-2017) along a chronosequence of fifteen peatlands, divided into three age classes, with the average values from both the 0-5 and 5-10 cm layers (n = 20 for each age class). The samples were from 0 - 10 cm below the average growing season ground water table. Thus even though the total age of the peatlands varied as indicated by the age classes, the absolute age of the peat in all these samples was on the order of decades. The "age" indicates the

457 amount time since the peat was established, during which time peat growth has separated the
458 superficial peat from the mineral substrate. Letters above boxes indicate significant differences (p
459 < 0.05) between the three age classes, classes with the same letter do not differ significantly.

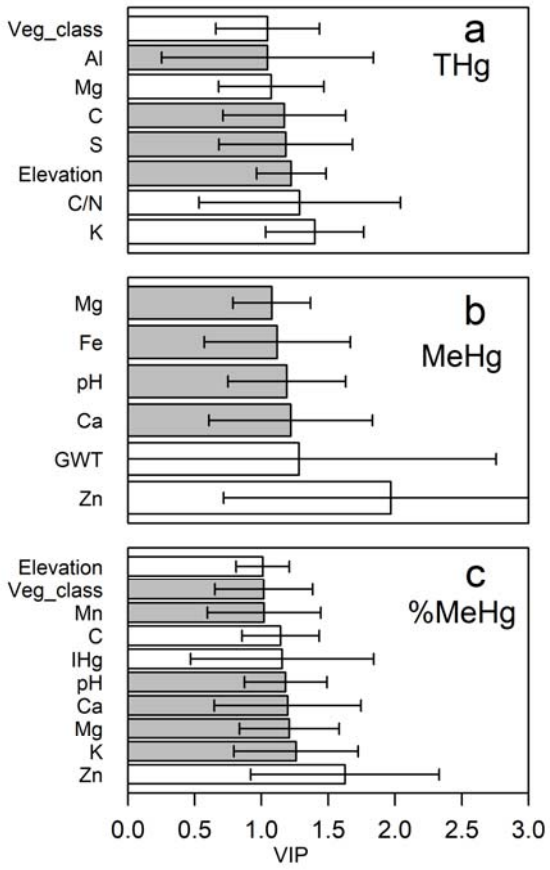

460

461 **Figure 4.** Major explanatory variables of PLS models with THg (a), MeHg (b) and %MeHg (c) as
462 dependent variables. The displayed variables are selected according to variable importance for the
463 projection (VIP > 1). Variables displayed with gray bars in each plot correlated positively with
464 corresponding independent variable, while unfilled bars correlated negatively.

Table 1. Characteristics of the study peatlands along the chronosequence

Peatland	Elevation (m.a.s.l)	Peat depth (cm)	Age (year)	N	E	Veg. Class[a]	pH[b]	Temp sum (°C)[c]		Precip (mm)[d]	
								2016	2017	2016	2017
02	0.72	70	72	63°51'3.90"	20°42'54.12"	6	5.0 ± 0.2	1308	1227	230	172
70	1.49	46	149	63°51'8.86"	20°42'35.14"	5	4.0 ± 0.2	1308	1227	230	172
43	3.43	70	341	63°52'11.67"	20°45'8.07"	3	4.0 ± 0.1	1307	1227	232	170
13	3.53	154	352	63°48'38.55"	20°34'51.54"	6	4.5 ± 0.1	1309	1228	223	170
10	5.07	140	503	63°49'9.09"	20°34'41.77"	6	4.1 ± 0.3	1309	1228	223	170
Y[e]	2.8 ± 1.6	98 ± 45	283 ± 154				4.3 ± 0.5	1308	1228	228	171
52	12.60	114	1221	63°57'16.73"	20°46'15.09"	4	4.7 ± 0.2	1300	1221	240	176
14	13.89	244	1341	63°50'54.39"	20°38'39.93"	3	4.5 ± 0.1	1302	1221	229	176
18	14.54	66	1401	63°53'8.15"	20°43'48.29"	4	3.6 ± 0.1	1298	1218	234	176
16	14.56	76	1402	63°52'47.97"	20°42'22.49"	2	3.9 ± 0.3	1298	1218	234	176
62	15.57	106	1495	63°50'37.38"	20°38'16.74"	1	3.8 ± 0.2	1302	1221	229	176
I[f]	14.2 ± 1.0	121 ± 72	1372 ± 90				4.1 ± 0.5	1300	1220	233	176
29	27.53	96	2547	63°52'52.61"	20°38'5.52"	1	3.7 ± 0.2	1296	1215	234	180
26	29.19	246	2686	63°52'5.08"	20°30'28.78"	1	3.7 ± 0.2	1303	1221	229	180
33	30.54	210	2799	63°54'17.68"	20°41'16.43"	2	3.9 ± 0.2	1298	1218	234	176
24	31.46	140	2874	63°51'31.51"	20°29'29.14"	1	3.8 ± 0.2	1303	1221	229	180
65	34.82	130	3146	63°52'58.48"	20°38'50.03"	1	3.8 ± 0.2	1296	1215	234	180
O[g]	30.7 ± 2.4	164 ± 61	2810 ± 200				3.8 ± 0.2	1299	1218	232	179

[a] Vegetation classes, from an initial survey of seventy peatlands along the chronosequence (data unpublished), with increasing number representing vegetation that requires more nutrients to thrive and spread.

[b] Mean pH ± SD of the four sampling occasions in 2016 and 2017.

[c] Sum of air temperatures during June, July and August in 2016 or 2017.

[d] Sum of precipitation during June, July and August in 2016 or 2017.

[c, d] Temperature and precipitation data is from www.smhi.se

[e, f, g] Rows represent average parameter values ± SD for young, intermediate and old peatland classes, respectively.

475 **Table 2.** Three-way ANOVA table for natural log transformed THg, MeHg and %MeHg of the 10
476 cm peat profile (divided into two 5 cm layers) immediately below the average growing season
477 ground water table in the three peatland age classes along a chronosequence of fifteen peatlands.
478 Boldface "Pr(> F)" indicates significance at $\alpha = 0.05$.

	Source of Variation	Df	Sum Sq	Mean Sq	F value	Pr(>F)
THg	Peatland age class [1]	2	7.60	3.802	24.53	**< 0.001**
	Month [2]	1	0.001	0.001	0.01	0.935
	Layer [3]	1	1.83	1.83	11.82	**< 0.001**
	Peatland age class × Month	2	0.21	0.11	0.68	0.507
	Peatland age class × Layer	2	0.21	0.11	0.68	0.508
	Month × Layer	1	0.004	0.004	0.02	0.877
	Peatland age class× Month × Layer	2	0	0	0	0.999
	Residuals	108	16.74	0.155		
	R squared = 0.37					
MeHg	Peatland age class	2	4.50	2.25	6.92	**0.002**
	Month	1	1.19	1.20	3.67	0.058
	Layer	1	3.26	3.26	10.01	**0.002**
	Peatland age class × Month	2	0.20	0.10	0.30	0.742
	Peatland age class × Layer	2	0.24	0.12	0.36	0.696
	Month × Layer	1	0.02	0.02	0.07	0.793
	Peatland age class× Month × Layer	2	0.10	0.05	0.15	0.859
	Residuals	108	35.13	0.33		
	R squared = 0.21					
%MeHg	Peatland type	2	23.62	11.81	31.34	**< 0.001**
	Month	1	1.13	1.13	3.00	0.086
	Layer	1	0.20	0.20	0.54	0.464
	Peatland age class × Month	2	0.28	0.14	0.38	0.687
	Peatland age class × Layer	2	0.12	0.06	0.16	0.857
	Month × Layer	1	0.01	0.01	0.02	0.883
	Peatland age class× Month × Layer	2	0.10	0.05	0.14	0.872
	Residuals	108	40.69	0.38		
	R squared = 0.38					

479 [1] Peatland age class = young, intermediate and old peatlands; [2] Sampling occasions in June and
480 August between 2016 and 2017; [3] Two layers (0-5 and 5-10 cm).
481

References

Åkerblom S, Bishop K, Björn E, Lambertsson L, Eriksson T, Nilsson MB. Significant interaction effects from sulfate deposition and climate on sulfur concentrations constitute major controls on methylmercury production in peatlands. Geochimica Et Cosmochimica Acta 2013; 102: 1-11.

AMAP. AMAP Assessment 2011: Mercury in the Arctic. Arctic Monitoring and Assessment Programme (AMAP) 2011.

Bae HS, Dierberg FE, Ogram A. Syntrophs dominate sequences associated with the mercury methylation-related gene hgcA in the water conservation areas of the Florida Everglades. Appl Environ Microbiol 2014; 80: 6517-26.

Benoit JM, Gilmour CC, Heyes A, Mason RP, Miller CL. Geochemical and Biological Controls over Methylmercury Production and Degradation in Aquatic Ecosystems. Biogeochemistry of Environmentally Important Trace Elements. 835. American Chemical Society, 2003, pp. 262-297.

Bergman I, Bishop K, Tu Q, Frech W, Akerblom S, Nilsson M. The Influence of Sulphate Deposition on the Seasonal Variation of Peat Pore Water Methyl Hg in a Boreal Mire. Plos One 2012; 7: 10.

Biester H, Hermanns Y-M, Martinez Cortizas A. The influence of organic matter decay on the distribution of major and trace elements in ombrotrophic mires – a case study from the Harz Mountains. Geochimica et Cosmochimica Acta 2012; 84: 126-136.

Branfireun BA, Bishop K, Roulet NT, Granberg G, Nilsson M. Mercury cycling in boreal ecosystems: The long-term effect of acid rain constituents on peatland pore water methylmercury concentrations. Geophysical Research Letters 2001; 28: 1227-1230.

Bravo AG, Zopfi J, Buck M, Xu J, Bertilsson S, Schaefer JK, et al. Geobacteraceae are important members of mercury-methylating microbial communities of sediments impacted by waste water releases. The ISME Journal 2018; 12: 802-812.

Compeau GC, Bartha R. Sulfate-Reducing Bacteria: Principal Methylators of Mercury in Anoxic Estuarine Sediment. Applied and Environmental Microbiology 1985; 50: 498-502.

Driscoll CT, Yan C, Schofield CL, Munson R, Holsapple J. The mercury cycle and fish in the Adirondack lakes. Environmental Science & Technology 1994; 28: 136A-143A.

Drott A, Lambertsson L, Björn E, Skyllberg U. Do Potential Methylation Rates Reflect Accumulated Methyl Mercury in Contaminated Sediments? Environmental Science & Technology 2008; 42: 153-158.

Fleming EJ, Mack EE, Green PG, Nelson DC. Mercury methylation from unexpected sources: molybdate-inhibited freshwater sediments and an iron-reducing bacterium. Appl Environ Microbiol 2006; 72: 457-64.

Gilmour CC, Henry EA, Mitchell R. Sulfate stimulation of mercury methylation in freshwater sediments. Environmental Science & Technology 1992; 26: 2281-2287.

Gilmour CC, Podar M, Bullock AL, Graham AM, Brown SD, Somenahally AC, et al. Mercury Methylation by Novel Microorganisms from New Environments. Environmental Science & Technology 2013; 47: 11810-11820.

Gilmour CC, Riedel GS, Ederington MC, Bell JT, Gill GA, Stordal MC. Methylmercury concentrations and production rates across a trophic gradient in the northern Everglades. Biogeochemistry 1998; 40: 327-345.

Hamelin S, Amyot M, Barkay T, Wang Y, Planas D. Methanogens: principal methylators of mercury in lake periphyton. Environ Sci Technol 2011; 45: 7693-700.

Haynes KM, Kane ES, Potvin L, Lilleskov EA, Kolka RK, Mitchell CPJ. Mobility and transport of mercury and methylmercury in peat as a function of changes in water table regime and plant functional groups. Global Biogeochemical Cycles 2017; 31: 233-244.

527 Hu H, Lin H, Zheng W, Rao B, Feng X, Liang L, et al. Mercury Reduction and Cell-Surface Adsorption by
528 Geobacter sulfurreducens PCA. Environmental Science & Technology 2013; 47: 10922-10930.
529 Hu H, Wang B, Bravo AG, Björn E, Skyllberg U, Amouroux D, et al. Shifts in mercury methylation across a
530 peatland chronosequence: From sulfate reduction to methanogenesis and syntrophy. Journal of
531 Hazardous Materials 2020; 387: 121967.
532 Hünicke B, Zorita E, Soomere T, Madsen KS, Johansson M, Suursaar Ü. Recent Change—Sea Level and
533 Wind Waves. In: The BIIAT, editor. Second Assessment of Climate Change for the Baltic Sea Basin.
534 Springer International Publishing, Cham, 2015, pp. 155-185.
535 Jeremiason JD, Engstrom DR, Swain EB, Nater EA, Johnson BM, Almendinger JE, et al. Sulfate Addition
536 Increases Methylmercury Production in an Experimental Wetland. Environmental Science &
537 Technology 2006; 40: 3800-3806.
538 Jiskra M, Wiederhold JG, Skyllberg U, Kronberg R-M, Hajdas I, Kretzschmar R. Mercury Deposition and Re-
539 emission Pathways in Boreal Forest Soils Investigated with Hg Isotope Signatures. Environmental
540 Science & Technology 2015; 49: 7188-7196.
541 Kerin EJ, Gilmour CC, Roden E, Suzuki MT, Coates JD, Mason RP. Mercury Methylation by Dissimilatory
542 Iron-Reducing Bacteria. Applied and Environmental Microbiology 2006; 72: 7919-7921.
543 Kodamatani H, Maeda C, Balogh SJ, Nollet YH, Kanzaki R, Tomiyasu T. The influence of sample drying and
544 storage conditions on methylmercury determination in soils and sediments. Chemosphere 2017;
545 173: 380-386.
546 Lambertsson L, Lundberg E, Nilsson M, Frech W. Applications of enriched stable isotope tracers in
547 combination with isotope dilution GC-ICP-MS to study mercury species transformation in sea
548 sediments during in situ ethylation and determination. Journal of Analytical Atomic Spectrometry
549 2001; 16: 1296-1301.
550 Loseto LL, Siciliano SD, Lean DR. Methylmercury production in High Arctic wetlands. Environ Toxicol Chem
551 2004; 23: 17-23.
552 Macdonald RW, Harner T, Fyfe J. Recent climate change in the Arctic and its impact on contaminant
553 pathways and interpretation of temporal trend data. Science of The Total Environment 2005; 342:
554 5-86.
555 McInerney MJ, Sieber JR, Gunsalus RP. Syntrophy in anaerobic global carbon cycles. Curr Opin Biotechnol
556 2009; 20: 623-32.
557 Mitchell CPJ, Branfireun BA, Kolka RK. Assessing sulfate and carbon controls on net methylmercury
558 production in peatlands: An in situ mesocosm approach. Applied Geochemistry 2008a; 23: 503-
559 518.
560 Mitchell CPJ, Branfireun BA, Kolka RK. Spatial Characteristics of Net Methylmercury Production Hot Spots
561 in Peatlands. Environmental Science & Technology 2008b; 42: 1010-1016.
562 Munthe J, Bodaly RA, Branfireun BA, Driscoll CT, Gilmour CC, Harris R, et al. Recovery of Mercury-
563 Contaminated Fisheries. Vol 36: BIOONE, 2007.
564 O'Callaghan JF, Mark DM. The extraction of drainage networks from digital elevation data. Computer
565 Vision, Graphics, and Image Processing 1984; 28: 323-344.
566 Osterwalder S, Bishop K, Alewell C, Fritsche J, Laudon H, Åkerblom S, et al. Mercury evasion from a boreal
567 peatland shortens the timeline for recovery from legacy pollution. Scientific Reports 2017; 7:
568 16022.
569 Ratcliffe HE, Swanson GM, Fischer LJ. Human exposure to mercury: a critical assessment of the evidence
570 of adverse health effects. J Toxicol Environ Health 1996; 49: 221-70.
571 Renberg I, Segerström U. The initial points on a shoreline displacement curve for southern Västerbotten,
572 dated by varve-counts of lake sediments. In: Königsson L-K, Paabo K, editors. Florilegium Florins
573 Dedicatum. 14. Striae, Uppsala, 1981, pp. 174-176.

574 Rydberg J, Karlsson J, Nyman R, Wanhatalo I, Näthe K, Bindler R. Importance of vegetation type for
575 mercury sequestration in the northern Swedish mire, Rödmossamyran. Geochimica et
576 Cosmochimica Acta 2010; 74: 7116-7126.
577 Schaefer JK, Morel FMM. High methylation rates of mercury bound to cysteine by Geobacter
578 sulfurreducens. Nature Geosci 2009; 2: 123-126.
579 St. Louis VL, Rudd JWM, Kelly CA, Beaty KG, Flett RJ, Roulet NT. Production and Loss of Methylmercury
580 and Loss of Total Mercury from Boreal Forest Catchments Containing Different Types of Wetlands.
581 Environmental Science & Technology 1996; 30: 2719-2729.
582 Stams AJM, Plugge CM. Electron transfer in syntrophic communities of anaerobic bacteria and archaea.
583 Nature Reviews Microbiology 2009; 7: 568-577.
584 Streets DG, Devane MK, Lu Z, Bond TC, Sunderland EM, Jacob DJ. All-Time Releases of Mercury to the
585 Atmosphere from Human Activities. Environmental Science & Technology 2011; 45: 10485-10491.
586 Tjerngren I, Karlsson T, Bjorn E, Skyllberg U. Potential Hg methylation and MeHg demethylation rates
587 related to the nutrient status of different boreal wetlands. Biogeochemistry 2012a; 108: 335-350.
588 Tjerngren I, Meili M, Bjorn E, Skyllberg U. Eight Boreal Wetlands as Sources and Sinks for Methyl Mercury
589 in Relation to Soil Acidity, C/N Ratio, and Small-Scale Flooding. Environmental Science &
590 Technology 2012b; 46: 8052-8060.
591 Tuittila E-S, Juutinen S, Frolking S, Väliranta M, Laine AM, Miettinen A, et al. Wetland chronosequence as
592 a model of peatland development: Vegetation succession, peat and carbon accumulation. The
593 Holocene 2013; 23: 25-35.
594 Wiatrowski HA, Ward PM, Barkay T. Novel Reduction of Mercury(II) by Mercury-Sensitive Dissimilatory
595 Metal Reducing Bacteria. Environmental Science & Technology 2006; 40: 6690-6696.
596 Windham-Myers L, Marvin-Dipasquale M, Krabbenhoft DP, Agee JL, Cox MH, Heredia-Middleton P, et al.
597 Experimental removal of wetland emergent vegetation leads to decreased methylmercury
598 production in surface sediment. Journal of Geophysical Research: Biogeosciences 2009; 114.
599 Wood JM, Kennedy FS, Rosen CG. Synthesis of methyl-mercury compounds by extracts of a methanogenic
600 bacterium. Nature 1968; 220: 173-4.
601 Yu R-Q, Flanders J, Mack EE, Turner R, Mirza MB, Barkay T. Contribution of coexisting sulfate and iron
602 reducing bacteria to methylmercury production in freshwater river sediments. Environmental
603 science & technology 2012; 46: 2684-2691.
604 Yu R-Q, Reinfelder JR, Hines ME, Barkay T. Syntrophic pathways for microbial mercury methylation. The
605 ISME Journal 2018; 12: 1826-1835.

606

Supplementary Information (SI) to

Opposing spatial trends in methylmercury and total mercury along a peatland chronosequence trophic gradient

Baolin Wang[1], Mats B. Nilsson[2], Karin Eklöf[1], Haiyan Hu[3, 4], Betty Ehnvall[2], Andrea G. Bravo [5], Shunqing Zhong[6], Staffan Åkeblom[1], Erik Björn[7], Stefan Bertilsson[1, 4], Ulf Skyllberg[2], Kevin Bishop[1]*

[1]Department of Aquatic Sciences and Assessment, Swedish University of Agricultural Sciences, SE-75007 Uppsala, Sweden.

[2]Department of Forest Ecology and Management, Swedish University of Agricultural Sciences, SE-90183 Umeå, Sweden.

[3]State Key Laboratory of Environmental Geochemistry, Institute of Geochemistry, Chinese Academy of Sciences, 550081 Guiyang, China.

[4]Department of Ecology and Genetics, Limnology and Science for Life Laboratory, Uppsala University, SE-75236 Uppsala, Sweden.

[5]Department of Marine Biology and Oceanography, Institut de Ciències del Mar (ICM-CSIC). Pg Marítim de la Barceloneta 37-49, E08003 Barcelona, Catalunya, Spain

[6]College of City and Tourism, Hengyang Normal University, 421002 Hengyang, China

[7]Department of Chemistry, Umeå University, SE-90187 Umeå, Sweden.

*Corresponding author, huhaiyan@mail.gyig.ac.cn

This supporting information contains 12 pages, 7 figures, and 3 tables.

Table of Contents

Figure S6: No differences in MeHg of the 10 cm peat profile among the three age groups between June (white) and August (gray) in 2016 (a), 2017 (b), and both 2016 and2017 (c). Letters above boxes indicate lack of significant differences ($p < 0.05$) between June and August, since boxes with the same letter do not differ significantly. n = 5 for each box in plot a and b, n = 10 for each box in plot c.

Figure S7: No differences in %MeHg of THg between June and August sampling occasions of each age group in the period of 2016, 2017, and both 2016 and 2017.

Table S1: Review of morphological and topographical indices as well as their interpretation.

Table ~~S3~~S2: Plant species characterizing the vegetation along a chronosequence of fifteen peatlands.

Table S3: Chemical parameters (mean ± SD) of the 10 cm layer below the water table in the three age groups along a chronosequence of fifteen peatlands.

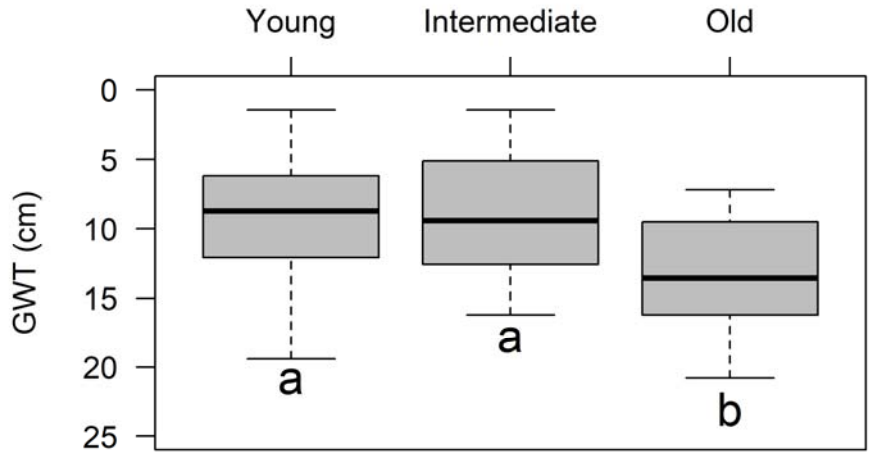

Figure S1. The ground water table (GWT) across the three age classes of peatlands on all four sampling occasions during 2016 and 2017. Letters above boxes indicate significant differences ($p < 0.05$) among the age classes, age classes with the same letter do not differ significantly. n = 100 for each age class.

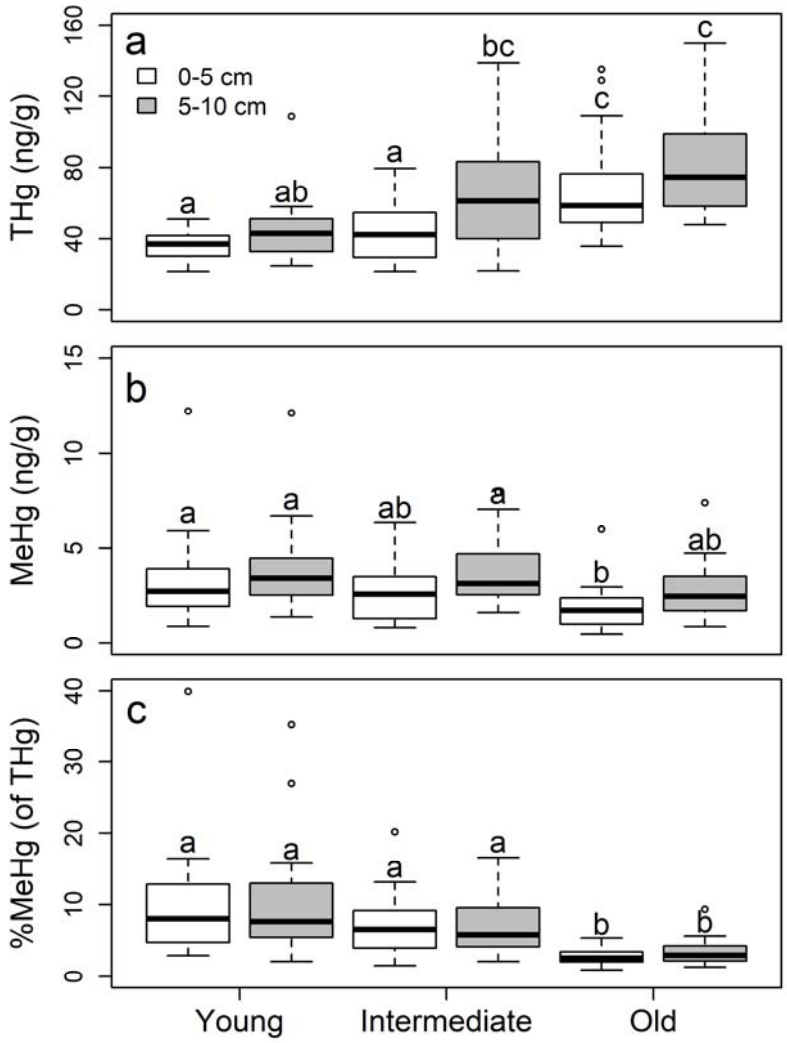

Figure S2. Concentrations of THg (a), MeHg (b), and %MeHg of THg (c) between 0-5 (white) and 5-10 cm (gray) layers among the three age groups of peatlands in the course of study from 2016 to 2017. Letters above boxes indicate significant differences ($p < 0.05$) between the layers, layers with the same letter do not differ significantly. n = 20 for each box in the plot.

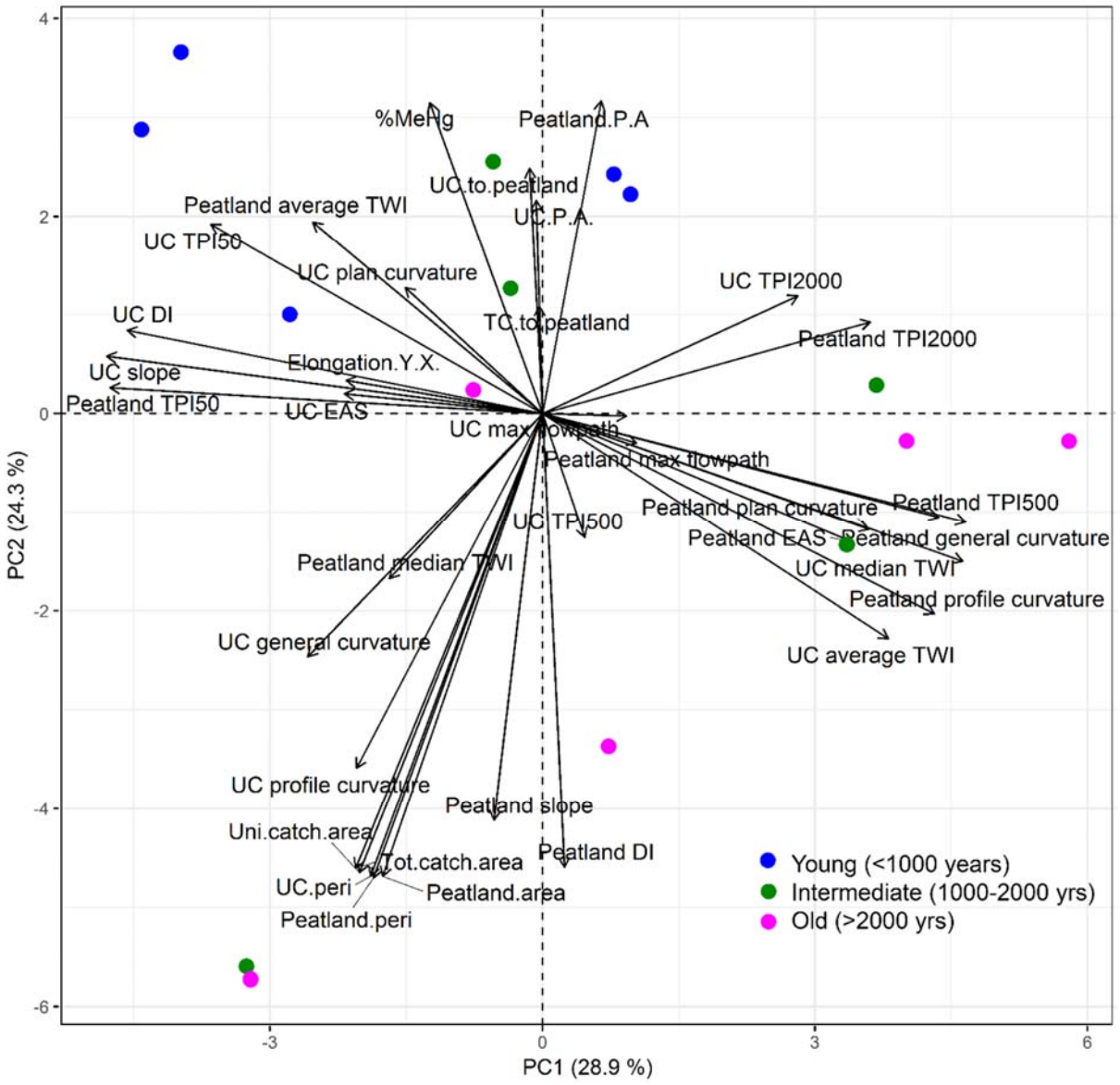

Figure S3. PCA of the topographic indices and average %MeHg of the two 5 cm layers of all the four samplings between 2016 and 2017. The three age classess can be separated in the PCA, where both hydrological and morphological features contribute to the separation due to peatland aging and landscape development.

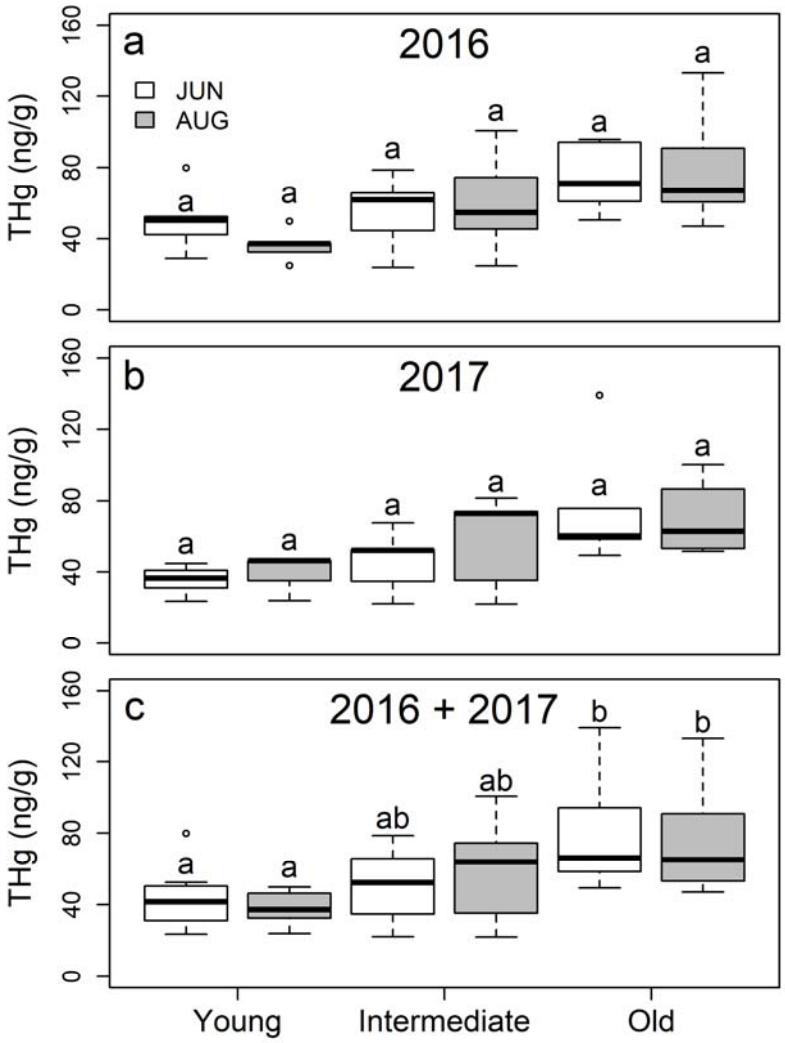

Figure S4. No differences in THg of the 10 cm peat profile among the three age groups between June (white) and August (gray) in 2016 (a), 2017 (b), and both 2016 and 2017 (c). Letters above boxes indicate significant differences ($p < 0.05$) between June and August, boxes with the same letter do not differ significantly. n = 5 for each box in plot a and b, n = 10 for each box in plot c.

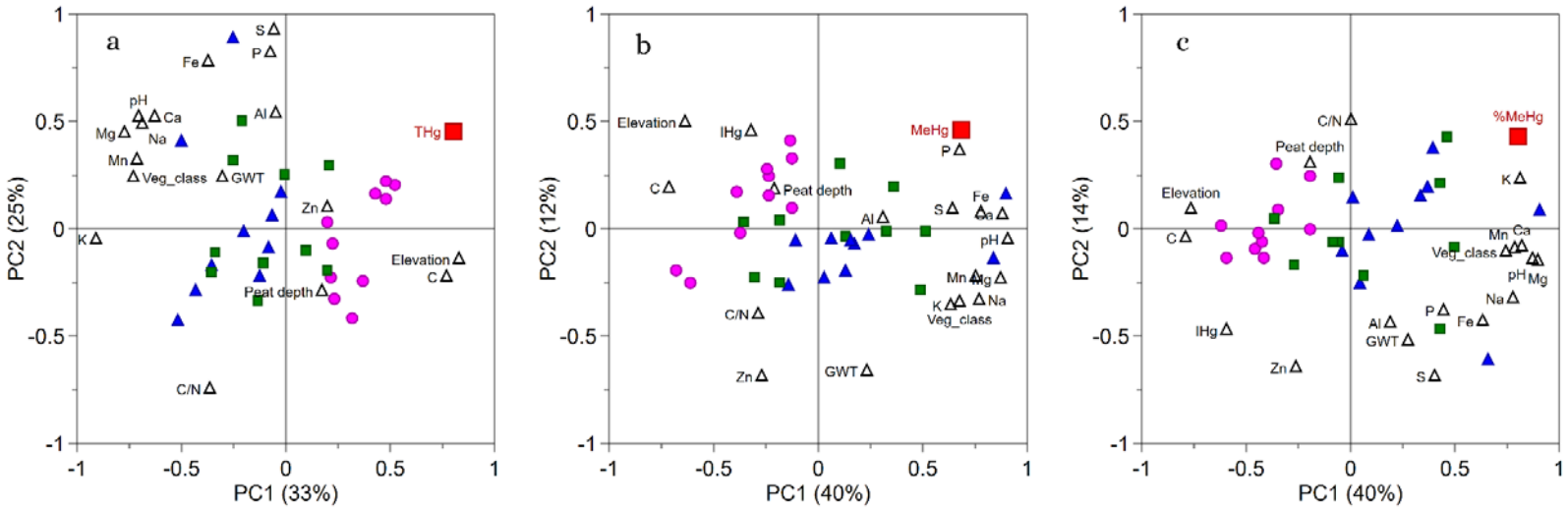

Figure S5. PLS analyses upon THg (a), MeHg (b) and %MeHg (c) along a chronosequence of fifteen peatlands in 2016. The fifteen peatlands were divided into three age classes according to peatland age, young (blue triangles), intermediate (green boxes) and old (pink dots).

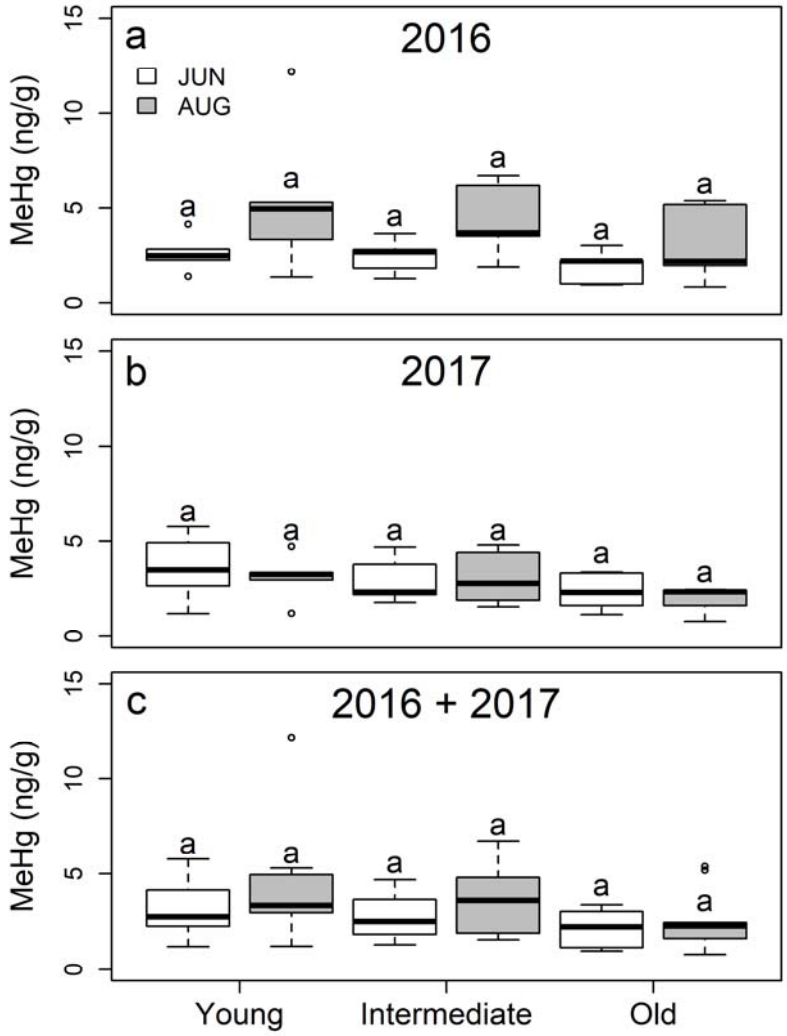

Figure S6. No differences in MeHg of the 10 cm peat profile among the three age groups between June (white) and August (gray) in 2016 (a), 2017 (b), and both 2016 and2017 (c). Letters above boxes indicate lack of significant differences ($p < 0.05$) between June and August, since boxes with the same letter do not differ significantly. n = 5 for each box in plot a and b, n = 10 for each box in plot c.

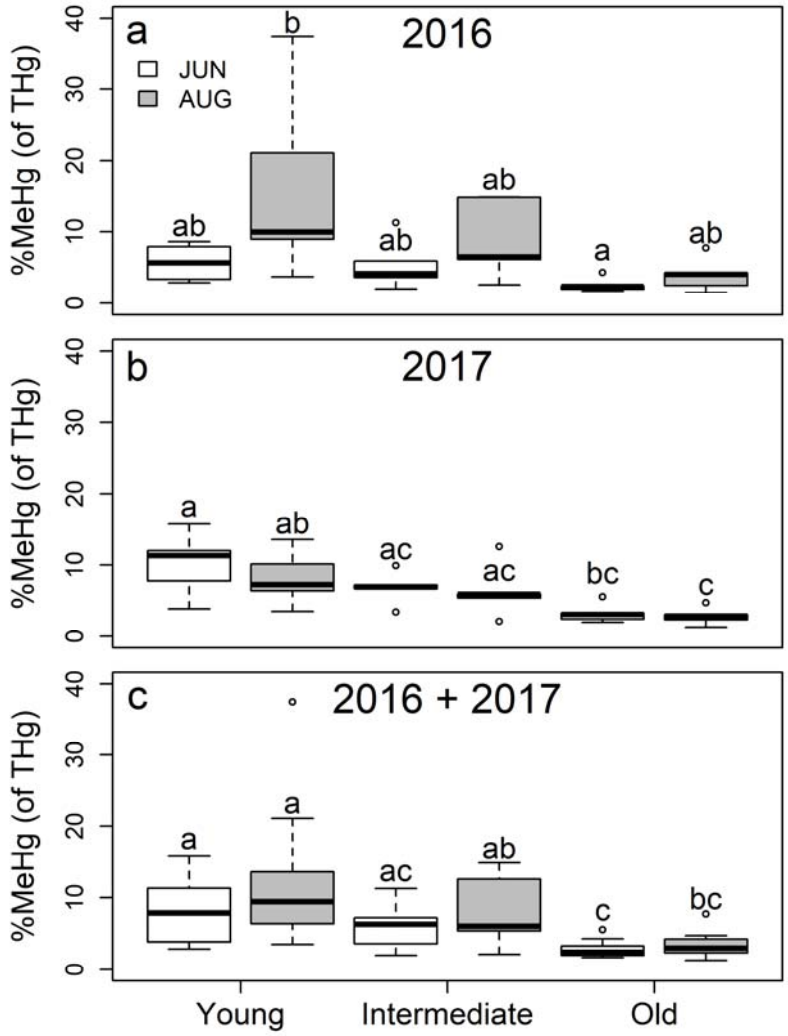

Figure S7. Differences in %MeHg of the 10 cm peat profile among the three age groups between June (unfilled) and August (gray) in 2016 (a), 2017 (b), and both 2016 and2017 (c). Letters above boxes indicate significant differences ($p < 0.05$) between June and August, boxes with the same letter do not differ significantly. n = 5 for each box in plot a and b, n = 10 for each box in plot c.

Table S1. Review of morphological and topographical indices as well as their interpretation. For raster based indices the accuracy is given.

Attribute	Description	Accuracy
Peatland.area.	peatland area	
Peatland.peri.	peatland perimeter	
Peatland.P.A.	peatland perimeter-to-area	
Elongation.Y.X.	peatland elongation calculated as $\Delta Y/\Delta X$.	
Tot.catch.area.	total hydrologically connected upslope area	2 m
Uni.catch.area.	peatland adjusted unique catchment area	2 m
TC.to.peatland	total catchment-to-peatland area ratio	
UC.to.peatland	unique catchment-to-peatland area ratio	
UC.peri.	Unique Catchment (UC) perimeter	
UC.P.A.	Unique Catchment perimeter-to-area ratio	
Peatland.elevation	peatland average elevation	2 m
Point.elevation	sampling point elevation	2 m
Peatland.age	peatland average age, based on DEM and site specific shore displacement curve	2 m
UC.age	UC average age, based on DEM and site specific shore displacement curve	2 m
Peatland_TPI50m	peatland topographic position index based on a 50 m neighbourhood size.	24 m
Peatland TPI500	peatland topographic position index based on a 500 m neighbourhood size.	24 m
Peatland TPI2000	peatland topographic position index based on a 2000 m neighbourhood size.	24 m
UC_TPI50m	peatland topographic position index based on a 50 m neighbourhood size.	24 m
UC TPI500	peatland topographic position index based on a 500 m neighbourhood size.	24 m
UC TPI2000	peatland topographic position index based on a 2000 m neighbourhood size.	24 m
Peatland.slope.	peatland slope (%)	2 m
UC.slope.	UC slope (%)	2 m
Peatland.DI	peatland downslope index, interpreted as the average hydraulic gradient of the peatland.	2 m
UC.DI	UC downslope index, interpreted as the average hydraulic gradient of the UC.	2 m
Peatland.EAS	elevation above stream, interpreted as the average peatland elevation above the water table.	2 m
UC.EAS	elevation above stream, interpreted as the average UC elevation above the water table.	2 m
Peatland.average.TWI	peatland topographic wetness index, interpreted as the average propensity of the peatland to be saturated to the soil surface.	24 m
UC.average.TWI	UC topographic wetness index, interpreted as the average propensity of the peatland to be saturated to the soil surface.	24 m
Peatland.median.TWI	peatland topographic wetness index, interpreted as the median propensity of the peatland to be saturated to the soil surface.	24 m
UC.median.TWI	UC topographic wetness index, interpreted as the median propensity of the peatland to be saturated to the soil surface.	24 m
Peatland_plan_curvature	peatland plan curvature; curvature perpendicular to the direction of the maximum slope.	2 m
Peatland_profile_curvature	peatland profile curvature; curvature parallel to the direction of the maximum slope.	2 m
Peatland_general_curvature	peatland general curvature; combination of peatland plan and profile curvature.	2 m
UC_plan_curvature	UC plan curvature; curvature perpendicular to the direction of the maximum slope.	2 m
UC_profile_curvature	UC profile curvature; curvature parallel to the direction of the maximum slope.	2 m
UC_general_curvature	UC general curvature; combination of UC plan and profile curvature.	2 m
Peatland_max_flowpath	maximum flow path length within the peatland	2 m
UC_max_flowpath	maximum flow path length before reaching the peatland edge	2 m

Table S2. Plant species characterizing the vegetation along a chronosequence of fifteen peatlands divided in to three age groups according to peatland age.

Peatland	Site	Characteristic plant species	
		Field-layer	**Ground-layer**
Young	02	*Potentilla palustris, Carex rostrata, Lysimachia thyrsiflora*	*Sphagnum squarrosum*
	70	*Carex limosa*	*Sphagnum fallax, Warnstorfia procera*
	43	*C. rostrata, Eriophorum angustifolium*	*Sphagnum majus, Sphagnum obtusum*
	13	*C. rostrata, Vaccinium oxycoccus, Epilobium palustre*	*S. fallax, Sphagnum riparium*
	10	*Carex magellanica, C. rostrata, P. palustris, V. oxycoccus*	*Sphagnum lindbergii, S. riparium*
Intermediate	52	*C. limosa, E. angustifolium*	*S. majus*
	14	*C. rostrata*	*S. lindbergii*
	18	*C. limosa, Scheuchzeria palustris*	*S. majus*
	16	*Carex lasiocarpa, Carex pauciflora, Eriophorum vaginatum, Trichophorum alpinum, Andromeda polifolia, V. oxycoccos*	*Sphagnum papillosum, S. majus*
	62	*E. vaginatum*	*S. papillosum, S. lindbergii*
Old	29	*C. pauciflora, E. vaginatum*	*Sphagnum balticum, S. majus, S. papillosum*
	26	*A. polifolia*	*S. majus, S. balticum*
	33	*T. alpinum, A. polifolia*	*S. majus, S. papillosum*
	24	*E. vaginatum, V. oxycoccus*	*S. balticum, S. majus, S. papillosum*
	65	*C. limosa, Trichophorum cespitosum*	*S. balticum, S. papillosum*

Table S3. Chemical parameters (mean ± SD) of the 10 cm layer below the water table in the three age groups along a chronosequence of fifteen peatlands in 2016 and/or 2017. n = number of samples for all parameters; parameters with n = 10 were only for samples in 2016, while parameters with n = 20 were for samples both in 2016 and 2017. Superscript letters along with values indicate significant differences ($p < 0.05$) among the three age groups, values with the same letter do not differ significantly.

Parameter	n	Peatland		
		Young	Intermediate	Old
pH	20	4.3 ± 0.5^{a}	4.1 ± 0.5^{a}	3.8 ± 0.2^{b}
THg (ng/g)	20	40.6 ± 12.9^{a}	54.5 ± 22.7^{a}	75.5 ± 26.7^{b}
MeHg (ng/g)	20	3.7 ± 2.4^{a}	3.2 ± 1.5^{ab}	2.3 ± 1.3^{b}
IHg (ng/g)	20	36.9 ± 13.4^{a}	51.3 ± 22.3^{a}	73.1 ± 26.1^{b}
%MeHg (%)	20	10.1 ± 7.9^{a}	6.9 ± 3.9^{a}	3.1 ± 1.6^{b}
C (%)	10	47.2 ± 1.3^{a}	47.3 ± 1.1^{a}	49.4 ± 1.4^{b}
N (%)	10	0.8 ± 0.4^{a}	0.8 ± 0.3^{a}	1.1 ± 0.4^{a}
C/N	10	66.3 ± 22.1^{a}	65.1 ± 24.3^{a}	50.5 ± 15.4^{a}
Al (mg/g)	10	1.2 ± 0.7^{a}	1.6 ± 0.9^{a}	1.0 ± 0.5^{a}
Ca (mg/g)	10	2.2 ± 0.6^{a}	2.3 ± 1.0^{a}	1.5 ± 0.6^{a}
Fe (mg/g)	10	3.8 ± 2.2^{a}	3.7 ± 1.3^{a}	2.1 ± 0.9^{b}
K (mg/g)	10	0.6 ± 0.3^{a}	0.5 ± 0.2^{a}	0.2 ± 0.1^{b}
Na (mg/g)	10	0.3 ± 0.28^{a}	0.2 ± 0.10^{a}	0.1 ± 0.04^{b}
Mg (mg/g)	10	1.1 ± 0.65^{a}	0.7 ± 0.28^{ab}	0.4 ± 0.07^{b}
Mn (mg/g)	10	0.022 ± 0.009^{a}	0.025 ± 0.011^{a}	0.012 ± 0.004^{b}
Zn (mg/g)	10	0.027 ± 0.009^{a}	0.025 ± 0.010^{a}	0.027 ± 0.011^{a}
S (mg/g)	10	2.6 ± 2.7^{a}	1.9 ± 1.4^{a}	1.8 ± 0.7^{a}
P (mg/g)	10	0.5 ± 0.2^{a}	0.4 ± 0.1^{a}	0.4 ± 0.1^{a}
Bulk density (g/cm^3)	10	0.02 ± 0.004^{a}	0.02 ± 0.01^{a}	0.03 ± 0.01^{a}